

The Performance Evaluation of Viscous-Modified Surfactant Waterflooding in Heavy Oil Reservoirs at Varying Salinity of Injected Polymer-Contained Surfactant Solution

Yadali Jamaloei, Benyamin*⁺

*Department of Chemical and Petroleum Engineering, Schulich School of Engineering,
University of Calgary, Calgary, AB, CANADA*

Kharrat, Riyaz

Petroleum Research Center, Petroleum University of Technology, Tehran, I.R. IRAN

ABSTRACT: *This study examines the effects of change in the concentrations of monovalent and divalent ions in the polymer-contained surfactant solution on the macroscopic behavior of viscous-modified surfactant waterflooding in heavy oil reservoirs. Salts that are used in this set of floods were sodium chloride, magnesium chloride, and calcium chloride. The results indicate that four different ranges of salinity (in terms of CaCl₂ concentration) exist. Each of these ranges renders a unique behavior regarding the ultimate oil recovery trends. There exists a range of salinity in which the ultimate oil recovery does not change with the salinity increase. The second salinity range is beyond the salt tolerance (i.e., first salinity range) of the polymer-contained surfactant solution, which results in a decrease in the ultimate oil recovery. In the third range of salinity, ultimate oil recovery is enhanced due to the plugging of high-permeable pores. In the fourth salinity range, precipitation increases as the salinity increases and more pore throats (even some pores with intermediate permeability) are plugged and, thus, the ultimate oil recovery decreases.*

KEY WORDS: *Viscous-modified surfactant waterflooding, Monovalent ions, Divalent ions, Micromodel, Heavy oil recovery.*

INTRODUCTION

The research on the use of surfactants to recover oil has extensively been carried since the 1930s. Patents and non-patent literature have conclusively shown that surfactant-based chemical solutions are capable of desaturating considerable trapped oil in the reservoirs

after initial waterflooding, if the chemical flood is properly tailored to the reservoir condition [1]. Several factors influence the surfactant-based chemical flooding processes. These factors include chemical types, chemistry of injected solution, phase behavior, adsorption, convection,

* To whom correspondence should be addressed.

+ E-mail: byadali@ucalgary.ca

1021-9986/12/1/99

13/\$/3.30

aging, stability, loss, dispersion, optimum formulation, wettability issues, pore morphology of the porous medium, etc. Effect of these parameters on the performance of surfactant-based chemical flooding has comprehensively been documented in the literature [2]. For a comprehensive literature survey, the reader is referred to the reviews provided by *Yadali Jamaloei* [1-2], *Yadali Jamaloei et al.* [3], *Yadali Jamaloei & Kharrat* [4-7], and *Yadali Jamaloei et al.* [8-11].

One of the limitations of the surfactant-based chemical flooding is the surfactant sensitivity to the reservoir environment, especially the surfactant sensitivity to the presence of divalent and monovalent ions. Here, the findings of some important studies are highlighted. Effects of divalent ions have been investigated by *Bansal & Shah* [12]. In particular, they reported an increase in IFT with increasing CaCl_2 (or MgCl_2) concentration in the connate water. *Bansal & Shah* [13] also noted that the optimum salinity (in terms of NaCl concentration) dropped as they increased the concentration of divalent ions. *Glover et al.* [14] pointed out that the optimal salinity is not constant in brines containing divalent ions and that phase trapping can result in large retention of surfactant in a system that was at optimal salinity at injected conditions. *Gupta et al.* [15] and *Glover et al.* [14] reported that the overoptimum salinity is not desirable in the drive water, as it may result in the surfactant partitioning into the trapped oil. *Hirasaki* [16] explained the displacement mechanisms that aided in the interpretation of salinity gradient. *Celik et al.* [17] reported that the interaction between the divalent ions and the petroleum sulfonates initially involved precipitation, followed by redissolution at higher surfactant concentrations. *Hirasaki & Lawson* [18] studied the association of surfactant micelles with sodium and calcium ions using electrostatic and equilibrium models. *Nelson* [19] showed that oil, not rock, plays the major role in trapping surfactant under high-salinity conditions. *Kumar et al.* [20] indicated that the IFT of dilute petroleum sulfonate solutions against oil increased dramatically upon additions of calcium or magnesium salts. *Kumar et al.* [21] documented the effects of divalent ions within the connate water on the coalescence behavior of oil droplets in surfactant formulations. They inferred that the addition of divalent cations to sodium-based petroleum sulfonate-lignosulfonate solutions strongly influenced

the coalescence of the oil droplets. Finally, *Maerker & Gale* [22] reasoned that lowering the drive-water salinity helps remobilizing part of the adsorbed surfactant.

The above literature survey shows that very little attempts have been carried out in the micromodels to visually study the behavior of surfactant-based chemical flooding. In the present work, a quarter five-spot etched-glass micromodel is used to probe into the effects of monovalent and divalent ions on the macroscopic behavior of the viscous-modified surfactant waterflooding. The foremost advantage of applying glass micromodel is its transparent feature that allows studying multiphase flow with the help of microscopy. Also, it is possible to have a more reliable determination of the physical properties of a micromodel as compared to those of real reservoir rocks. The latter allows a more efficient quantification of the flow characteristics which are difficult, or even impossible, to determine in the reservoir rocks. Additionally, no works have been reported in the literature for examining the effects of monovalent and divalent ions in the surfactant-polymer solution on the dynamics of the viscous-modified surfactant waterflooding, i.e., change in the ratio of viscous-to-capillary forces (capillary number). This study examines the above-mentioned issues, which are missing from the literature. The influence of monovalent and divalent ions on the IFT, viscosity, and the capillary number in both waterflooding and viscous-modified surfactant waterflooding is evaluated. The change in the capillary number in both waterflooding and viscous-modified surfactant waterflooding are used to evaluate the dynamics of both processes in a porous network filled with connate water and heavy oil. Furthermore, utilizing micromodel in this study, the interactions between the surfactant and the monovalent and divalent ions in the surfactant solution are observed. The precipitation and the pore blockage phenomenon as a result of the incompatibility between the surfactant and calcium chloride are observed in some concentration ranges of the calcium chloride. The results of this fundamental study reveal that some unusual events such as the pore blockage phenomenon (due to the physicochemical interactions between the surfactant and calcium chloride in the injected solution) may significantly influence the trend of heavy oil recovery during viscous-modified surfactant waterflooding. In addition, under the experimental conditions in this study, the effect of

Table 1: Properties of the petroleum sulfonate.

Approximate Equivalent Weight	Active Sulfonate Content (wt.%)	Free oil (wt.%)	Water (wt.%)	Inorganic Salts (wt.%)
380	54	16.1	17.8	3.3

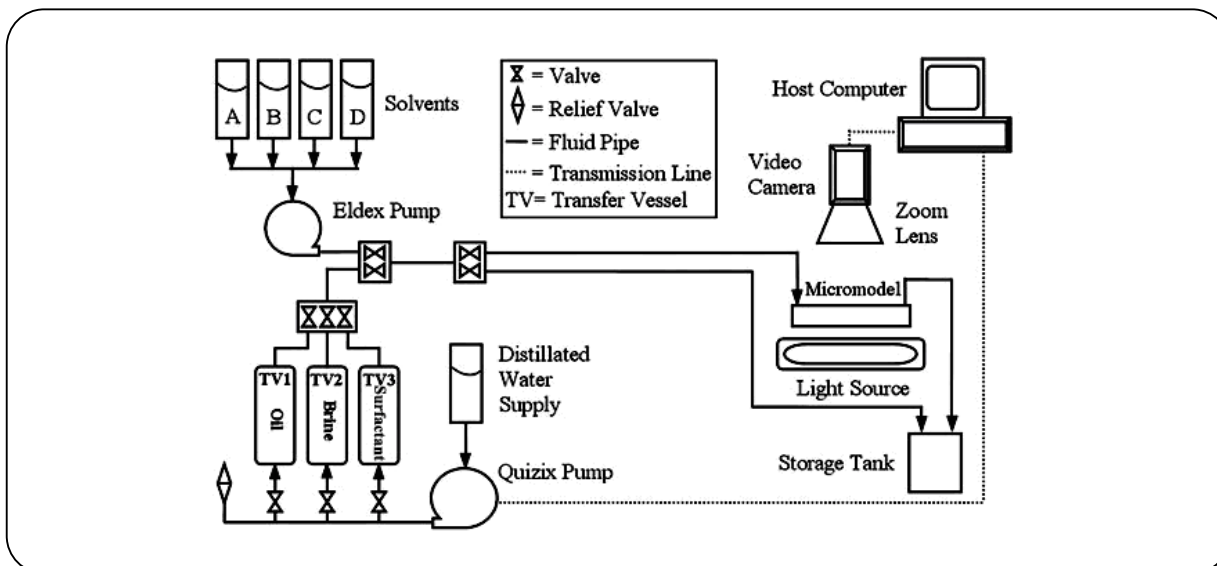


Fig. 1: Schematic of micromodel set-up (© 2008 Society of Petroleum Engineers, reproduced from Ref. [32] with permission of the copyright owner. Further reproduction prohibited without permission)

wettability alteration on the trend of heavy oil recovery during the viscous-modified surfactant waterflooding is relatively minor as compared to the effect of pore blockage. The presented results in this study help to provide a more realistic picture of the viscous-modified surfactant waterflooding in heavy oil reservoirs.

EXPERIMENTAL SECTION

Set-up description

Fig. 1 shows a schematic diagram of the experimental set-up. The micromodel set-up consists of cleaning system, fluid injection section, optical system, photography system, micromodel holder, and the monitoring computer system. High-precision Quizix model micro flow piston pump (positive displacement, stepper motor-driven pump, QL-700 Pump) can inject the displacing fluid with an injection rate between 10^{-5} and $10 \text{ cm}^3/\text{min}$. Camera can be moved horizontally and it is capable of working at a magnification up to 200 times. Pump supply, transfer vessels, pump pressure supply, Eldex pump, and filter are other parts of the set-up.

Materials

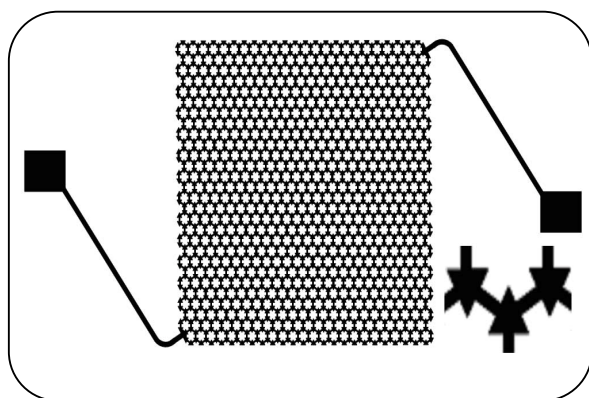
The properties of the surfactant material are given in Table 1. The active concentration of surfactant in the polymer-contained surfactant solution is constant (0.10 wt.%) in all the tests, which is below the critical micelle concentration (0.90 wt.%) of the surfactant. To avoid severe viscous fingering, xanthan polymer (supplied by the Research Institute of Petroleum Industry, Tehran, Iran) with a concentration of 125 ppm was added to the dilute surfactant solution. Ethanol (supplied by Merck, Germany, purity of 99.8%) was used in the polymer-contained surfactant solution to minimize surfactant adsorption [5, 6, 23]. Ethanol was used (0.75 wt.%) in the surfactant solution since the adsorption of some surfactants can be reduced by the addition of low-molecular-weight alcohols [23]. To minimize surfactant adsorption, surfactant adsorption tests were carried out in the absence of oil to ensure that the retained surfactant is due to adsorption and not due to the partitioning into the oil [5, 24]. Further details on surfactant adsorption tests can be found in Ref. [5]. West Paydar heavy oil (West Paydar is an oil field in west of Iran) has been

Table 2: Properties of the crude oil.

Temperature (°C)	Density (kg/m ³)	Viscosity (mPa·s)
15.5	933.2	142.01
21	929.9	101.77

Table 3: Physical and hydraulic properties of glass micromodel.

Pore shapes	Pore diameter (μm)	Throat diameter (μm)	Coordination number	Aspect ratio	Absolute permeability (m ²)	Porosity (Fraction)	Average etched thickness (μm)
Triangle	647±25	280±15	3	2.31	$(2.35 \pm 0.3) \times 10^{-12}$	0.4082	29

**Fig. 2: A schematic of one-quarter five-spot glass micromodel with a magnified view of its pores.**

used as the oil. The density and viscosity of the crude oil at different conditions (see Table 2) were measured using a digital densitometer (512P, Anton Paar[®]) and a rolling-ball viscometer (P/N, Chandler Engineering), respectively. NaCl, MgCl₂, and CaCl₂ were supplied by Merck, Germany, with the purities of 99.5%, 98% and 99.9%, respectively. Hydrofluoric acid (40%, supplied by Merck, Germany) and nitric acid (Suprapur grade, supplied by Merck, Germany) were used to etch the porous network onto the glass. The viscosity of the polymer-contained surfactant solution was measured by a capillary viscometer. Contact angles were measured on the glass and the micromodel was identified as water-wet. For instance, the measured contact angle for brine with C_n = 1.8 wt.%, C_m = 1.2 wt.%, and C_c = 0.6 wt.% was 7.4°. The contact angle for brine with C_n = 1.8 wt.%, C_m = 1.8 wt.%, and C_c = 1.8 wt.% changed to 9.7°. All the measurements and experiments were conducted at a temperature of 26 °C.

Procedures

First, pattern of the synthetic porous medium

is designed using Freehand Graphics and CorelDraw Graphics. Then, it is etched onto the glass utilizing an especial etching technique. A schematic of the pattern is given in Fig. 2. After the etching, micromodel patterns are fused in a special oven (Blue M Standard Ultra-Temp[®] High-Temperature) so as to create a homogeneous etched depth throughout the entire pattern. Further details on fusing and etching procedures can be found elsewhere [2].

Physical and hydraulic properties of the micromodels are given in Table 3. Uniform pore and throat diameters cannot be etched through the entire porous network. Therefore, actual etched pore body and throat diameters along with their fluctuation have been measured. The fluctuation in the etched throat and pore diameters in the micromodel was found as $\pm 15 \mu\text{m}$ and $\pm 25 \mu\text{m}$, respectively. The coordination number in Table 3 is the number of pore necks connected to a single pore body. The aspect ratio is the ratio of pore-to-throat diameter. In addition, the length and width of the micromodel is 60 mm. The absolute permeability of the micromodel was measured by recording pressure drops at various flowrates and using Darcy's law [5, 6, 25, 26]. The micromodel porosity was determined using image analysis [6]. Finally, etched depth of the micromodel was measured utilizing a depth measurement apparatus (Mitutoyo (NO3109F)). It is worth noting that in order to some extent simulate the roughness of a reservoir rock- which affects the contact angle distribution throughout a porous medium [27, 28]- a micromodel with considerably rough pore walls is used here. Images of micromodels with different roughness on their pore walls are given in Yadali Jamaloei & Kharat [7].

To start each test, first, brine with a constant salinity (NaCl concentration = 1.0 wt.%, MgCl₂ concentration = 0.50 wt.%, CaCl₂ concentration = 0.50 wt.%) is injected into the micromodel. Then, West Paydar crude oil

is injected to displace the brine so as to establish the condition of connate water saturation within micromodel. Then, brine, and consequently, polymer-contained surfactant solution are injected at a constant injection flowrate of 0.0006 cm³/min. Fluids injection procedures used here are the widely-accepted procedures in the literature [29-31]. To clean the micromodel after each experiment, first, micromodel is washed with toluene followed by rinsing with ethanol. This procedure is repeated until micromodel is restored to its original, clean state when it is ready to do the next experiment.

A high-resolution camera captured high-quality images during the displacement in the micromodel. The captured images are then loaded into SigmaScan Pro 5.0[®] for the analysis. After the image analysis, quantities like oil recovery and residual oil saturation at any time are determined. To investigate the repeatability of the results, some experiments were repeated. In general, ultimate oil recoveries slightly changed, but the trends remained unchanged. Thus, the repeatability of the results was acceptable.

RESULTS AND DISCUSSION

In three sets of experiments, the effect of Ca²⁺ at three concentrations of Mg²⁺ is studied. For each concentration level of MgCl₂ (1.2, 1.8 and 2.4 wt.%), the concentration of CaCl₂ in the polymer-contained surfactant solution is increased from 0.6 to 2.6 wt.% by increments of 0.2. In these three sets, concentration of NaCl (1.8 wt.%) is constant. IFTs between the crude oil and the polymer-contained surfactant solution and also the solution density at different salinities are measured. The ultimate oil recovery at different salinities is also determined.

In the fourth set of runs, the effect of Na⁺ at the given concentration of Mg²⁺ and Ca²⁺ is studied. The concentration of NaCl within the polymer-contained surfactant solution is increased from 2 to 2.8 wt.% by increment of 0.2 when concentrations of MgCl₂ and CaCl₂ (0.5 wt.%) are constant. In this set, IFTs between the pairs of crude oil-surfactant solution, the crude oil-brine, surfactant solution density, and ultimate oil recovery at different concentrations of Na⁺ are measured.

The following definition of the capillary number N_c is used in this study in order to characterize the dynamics of the waterflooding and the viscous-modified surfactant waterflooding at different concentrations of monovalent and divalent ions:

$$N_c = \frac{\text{Displacing fluid dynamic viscosity (Pa} \cdot \text{s)} \times \text{Displacing fluid velocity (m/s)}}{\text{Interfacial tension (N/m)} \times \text{Contact angle (}^\circ\text{)}}$$

The above definition is used to determine N_c and to plot Figs. 7, 8 and 13. As the above relationship shows, the capillary number is a dimensionless number that expresses the ratio of viscous-to-capillary forces. The value of capillary number is set by the displacing fluid dynamic viscosity, displacing fluid velocity, IFT between the two phases, and the contact angle.

Effect of divalent ions (Ca²⁺, Mg²⁺)

Ultimate oil recovery values for the initial waterflooding and consequent viscous-modified surfactant waterflooding versus CaCl₂ concentration at different concentrations of MgCl₂ are given in Fig. 3. To confirm these trends, some experiments were repeated and their repeatability was fairly acceptable (relative error in the range of 1–2%).

As it is shown in Fig. 3, ultimate oil recovery values for the waterflooding do not change noticeably by increasing CaCl₂ concentration (for MgCl₂ concentration of 1.2 wt.%). This trend is the same for the higher concentrations of MgCl₂ (1.8, 2.4 wt.%). In all these experiments no precipitation occurred as brines with different salinities were injected into the micromodel. As it is shown in Fig. 4, IFT between brine and crude oil increases by the increase in CaCl₂ concentration for all the concentrations of MgCl₂ (1.2, 1.8 and 2.4 wt.%). At intermediate concentrations of CaCl₂ (1–1.6 wt.%), increase in IFT values by increase in the MgCl₂ concentrations (1.8, 2.4 wt.%) is negligible. However, at low and high concentrations of CaCl₂ (0.6–1 wt.% and 1.6–2.6 wt.%, respectively), increase in brine-oil IFT by increasing MgCl₂ concentration is noticeable. Notwithstanding the increase in brine-oil IFT by increasing the CaCl₂ concentration for each MgCl₂ concentration level (Fig. 4), waterflooding recovery did not change considerably (Fig. 3). This is attributed to the fact that by increasing CaCl₂ concentration in brine, brine viscosity also increases (see Fig. 5). By the increase in brine viscosity, waterflooding front becomes more stable. This tends to increase the sweep efficiency. On the other hand, increasing CaCl₂ concentration increases the brine-oil IFT, which tends to lower displacement efficiency. These two effects cancel each other out. Hence, no remarkable change in the waterflooding recovery

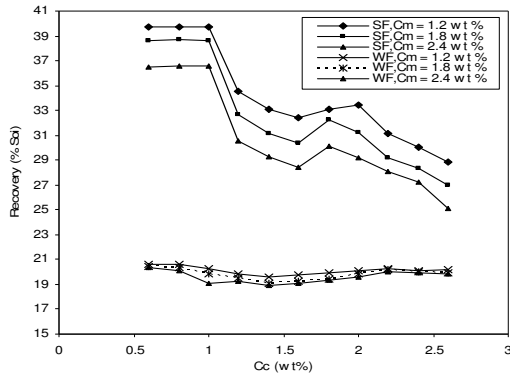


Fig. 3: Ultimate oil recovery values in waterflooding and viscous-modified surfactant waterflooding for different salinities of the brines and polymer-contained surfactant solution. Concentrations of chemicals in polymer-surfactant solution in surfactant waterfloods are: surfactant = 0.10 wt.%, xanthan = 125 ppm, and ethanol = 0.75 wt.%.

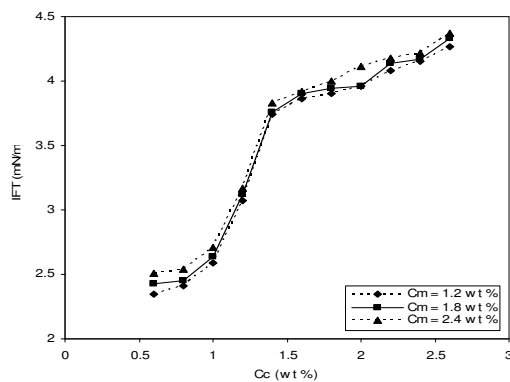


Fig. 4: IFT between brine and oil versus CaCl_2 concentration for three concentrations of MgCl_2 .

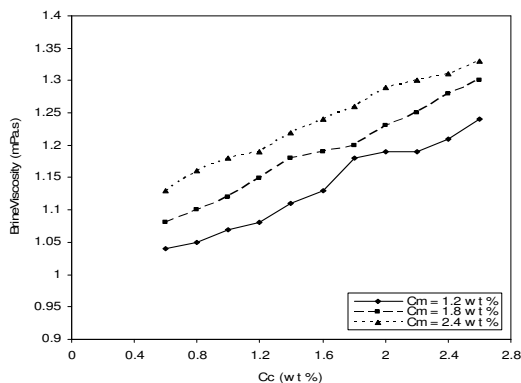


Fig. 5: Measured brine viscosity versus CaCl_2 concentration for three concentrations of MgCl_2 .

is observed by the increase in CaCl_2 concentration for three different MgCl_2 concentrations (Fig. 3).

Regarding the oil recovery trends in the viscous-modified surfactant waterflooding (Fig. 3), different CaCl_2 concentration ranges exist. Based on the results in Fig. 3, four different ranges of CaCl_2 concentration exist (for each level of MgCl_2 concentration: 1.2, 1.8, 2.4 wt.%). Each of these ranges renders a unique behavior considering the ultimate oil recovery trends.

Surfactant solution–oil IFTs are given in Fig. 6. IFT between the polymer-contained surfactant solution and the oil increases by the increase in CaCl_2 concentration in a given concentration of MgCl_2 . Fig. 6 shows that at higher concentrations of CaCl_2 (1.6–2.6 wt.%) increase in IFT is sharper when MgCl_2 concentration increases from 1.2 to 2.4 wt.%. Hence at higher concentrations of CaCl_2 , IFT values become more sensitive to the increase in MgCl_2 concentration. Fig. 6 also shows that at intermediate CaCl_2 concentration (1–1.6 wt.%), IFT values increase sharply for all the levels of MgCl_2 concentration (1.2, 1.8 and 2.4 wt.%). This is the reason for the sudden decrease in ultimate oil recovery in the second range in Fig. 3.

Fig. 3 shows that there is a range of CaCl_2 concentration ($C_c = 0.6$ –1 wt.%) in which the surfactant performance is not adversely affected and the ultimate oil recovery does not change with increase in CaCl_2 concentration. This range of CaCl_2 concentration ($C_c = 0.6$ –1 wt.%) is called the optimum range. In optimum range, IFTs and capillary numbers do not change by the increase in CaCl_2 concentration (Figs. 6 and 7). This concentration range is the range of CaCl_2 concentration tolerance for the viscous-modified surfactant waterflooding tests. In this optimum range, no sign of precipitation and plugging in the micromodel was observed. To be precise, no injection pressure peaks in the Quizix pump datalog was detected. Also, visual inspection of the micromodel under a high-resolution camera did not reveal the presence of any precipitate in the micromodel.

As CaCl_2 concentration in the injected polymer-contained surfactant solution increases, oil recovery decreases abruptly (second CaCl_2 concentration range in Fig. 3: 1–1.6 wt.%). This is attributed to the increase in IFT by increasing CaCl_2 concentration. The values of IFT and capillary number for this range are given in Figs. 6 and 8,

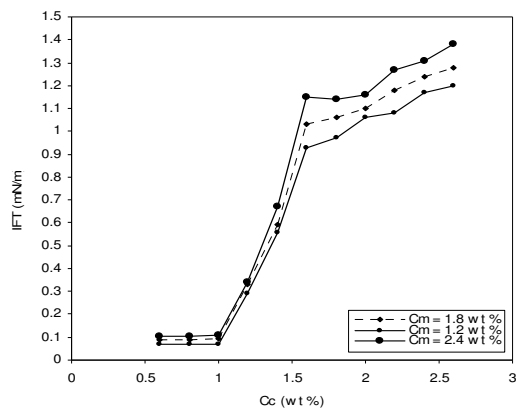


Fig. 6: IFT between polymer-contained surfactant solution and oil versus CaCl_2 concentration for three concentrations of MgCl_2 . Concentrations of chemicals in polymer-surfactant solution in surfactant waterfloods are: surfactant = 0.10 wt.%, xanthan = 125 ppm, and ethanol = 0.75 wt.%.

respectively. It is worth mentioning that in this CaCl_2 concentration range, no signs of precipitation and pore plugging in the micromodel were observed. This CaCl_2 concentration range is beyond the tolerance range (first CaCl_2 concentration range) of the polymer-contained surfactant solution.

The above trend does not continue by further increase of CaCl_2 concentration. After CaCl_2 concentration reaches a certain value (i.e., 1.6 wt.%), ultimate oil recovery starts to increase (see Fig. 3: third CaCl_2 concentration range). However, oil recovery values in this range do not reach those of the first range (0.6–1.0 wt.%). At MgCl_2 concentration of 1.2 wt.%, third concentration range for CaCl_2 lies between 1.6–2 wt.%. At higher concentrations of MgCl_2 (1.8 and 2.4 wt.%), third range of CaCl_2 concentration is shortened (1.6–1.8 wt.%). In the third range, when CaCl_2 concentration increases in the surfactant solution, precipitates start to locally form in some portions of the micromodel. These precipitates plug some high-permeable portions and, thus, divert the flow of surfactant solution to the intermediate-permeable portions. This causes sweeping of the intermediate-permeable parts. This is the reason for the higher ultimate oil recoveries in the third range than those in the second range despite the existence of higher IFTs and lower capillary numbers in the former range (see Figs. 6 and 8). Portions with different permeabilities in the micromodel exist because there are some pores, which may fluctuate in throat diameter.

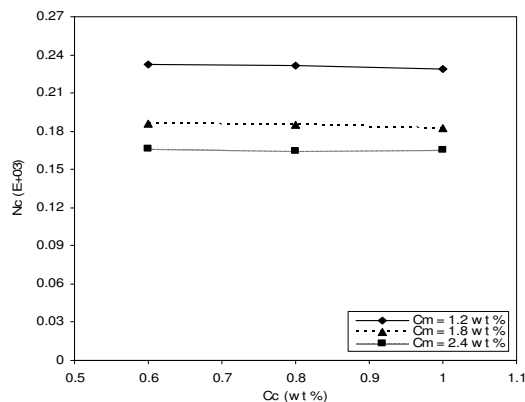


Fig. 7: Capillary number in viscous-modified surfactant waterflooding versus CaCl_2 concentration (first range) for three concentrations of MgCl_2 . Concentrations of chemicals in polymer-surfactant solution in surfactant waterfloods are: surfactant = 0.10 wt.%, xanthan = 125 ppm, and ethanol = 0.75 wt.%.

The fluctuation of throat diameter is allotted to the etching procedure. It is worth citing that in this CaCl_2 concentration range, IFT increases by increasing CaCl_2 concentration (see Fig. 6). Hence the increase in the ultimate oil recovery in the third range of CaCl_2 concentration is because of the plugging of some high-permeable pores throats (i.e., pore blockage phenomenon).

The onset and symptoms of precipitation were identified in the micromodel under a digital camera. Also, the mechanism of forming and the nature of precipitate were identified using some precipitation tests after the observation of pore blockage in the micromodel. It is worth citing that the precipitation tests were not conducted prior to the surfactant waterflooding experiments. The formation of this precipitate is allotted to the interaction of the surfactant as the polymer-contained surfactant solution contacts some pores that contain sufficient concentrations of Ca^{2+} in the micromodel. The mechanism of forming and the nature of this precipitate together with the consequent plugging of some pores in the micromodel are explained here. To explain the behavior of the third range of CaCl_2 concentration and to identify the mechanism responsible (i.e., pore blockage phenomenon) for the increase in oil recovery in this range, several precipitation tests involving surfactant and the divalent ions were conducted. The results indicate that a sticky precipitate forms, deposits, and adheres to the glass in this

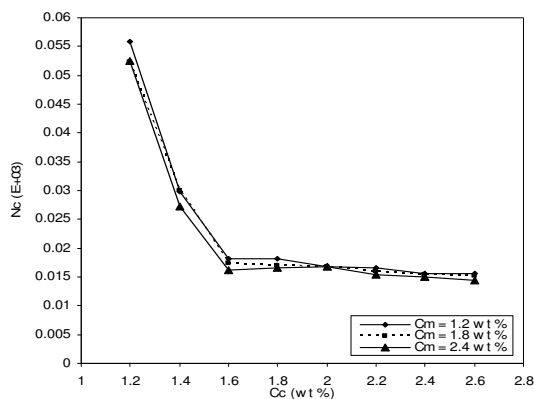


Fig. 8: Capillary number in viscous-modified surfactant waterflooding versus CaCl_2 concentration (2nd, 3rd, 4th ranges) for three concentrations of MgCl_2 . Concentrations of chemicals in polymer-surfactant solution in surfactant waterfloods are: surfactant = 0.10 wt.%, xanthan = 125 ppm, and ethanol = 0.75 wt.%.

concentration range of CaCl_2 and MgCl_2 (CaCl_2 concentration = 1.6–2 wt.% when MgCl_2 concentration = 1.2–2.8 wt.%). Microscopic evaluations of the captured images (for instance, see Fig. 15) showed that solids do not exist in this sticky precipitate. Thus, the mechanism of precipitation and pore blockage can now be explained after observing the sticky precipitate formed during the precipitation tests. During the waterflooding, some pores adsorb a sufficient concentration of Ca^{2+} that is present in the brine used in the early waterflooding experiments. It is noted that the connate water does not contain sufficient concentration of Ca^{2+} . Afterwards, the injected polymer-contained surfactant solution initially tends to flow through these zones that have less resistance to flow. These zones with less resistance had previously been developed because of the brine flow during the early waterflooding. The pores in these zones are now enriched in Ca^{2+} after the waterflooding. Hence, the injected surfactant solution contacts the mentioned pores, which are now enriched in Ca^{2+} . Consequently, a precipitate is formed in these pores as a result of the interaction of surfactant with Ca^{2+} . Thus, these pores are blocked with a sticky precipitate observed during the precipitation tests (i.e., as a result, no or a partial flow would take place through the blocked pores). Afterwards, the bulk flow of the surfactant solution is preferentially diverted into the previously-unswept portions with intermediate-to-high resistance to flow. This preferential flow of the surfactant

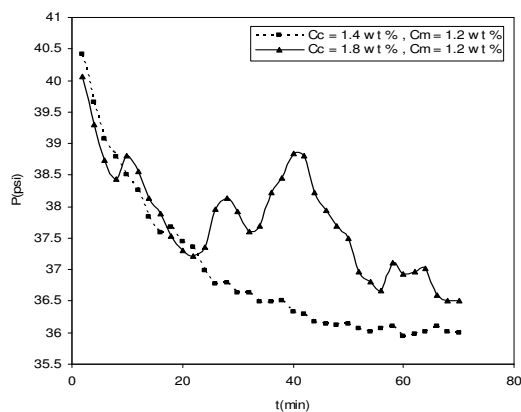


Fig. 9: A typical injection pressure response versus time in the third range of CaCl_2 concentration during the viscous-modified surfactant waterflooding of a porous network filled with connate water and heavy oil.

solution into the previously-unswept portions significantly enhances the ultimate oil recovery in the third range of CaCl_2 concentration. The evidence of precipitation in the glass micromodel has been given in Fig. 15. Additionally, another sign of precipitation is witnessing some peaks in the injection pressure response at/close to the precipitation times. The injection pressure was continuously recorded in the Quizix pump data log. The recorded log of the injection pressure of the surfactant solution (Fig. 9) shows some instantaneous peaks when precipitates locally block some pores or when they start to locally form in the micromodel. A typical injection pressure response at the time of precipitation and plugging is given in Fig. 9.

After the third range of CaCl_2 concentration, precipitation increases in such a way that more pore throats (even some of the pores with intermediate permeability) are plugged. Thus, the ultimate oil recovery decreases as CaCl_2 concentration increases (see the fourth range in Fig. 3). The decrease of ultimate oil recovery values in the fourth range are attributed to the: (i) increase in IFT (Fig. 6), (ii) decrease in capillary number (Fig. 8), and (iii) plugging of some high- and intermediate-permeable pores. This range is the fourth CaCl_2 concentration range (2–2.6 wt.%). The nature of precipitate formed and its mechanism of formation in the fourth range of CaCl_2 concentration are similar to those observed in the third range. Moreover, the increasing

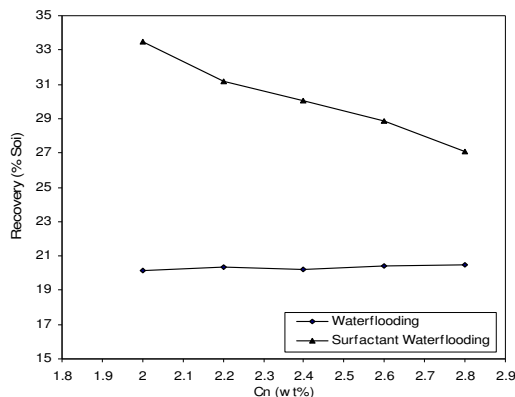


Fig. 10: Ultimate oil recovery in waterflooding and viscous-modified surfactant waterflooding versus NaCl concentration ($MgCl_2 = 0.5$ wt.%, $CaCl_2 = 0.5$ wt.%). Concentrations of chemicals in polymer-surfactant solution in surfactant waterfloods are: surfactant = 0.10 wt.%, xanthan = 125 ppm, and ethanol = 0.75 wt.%.

values of the IFT (see the last part of the Fig. 6) in this range played another role in the decreasing values of the ultimate oil recovery.

In summary, based on the analysis provided, a tolerance range for the polymer-contained surfactant solution is distinguished (first range of $CaCl_2$ concentration: 0.6–1 wt.%) beyond which the ultimate oil recovery of surfactant waterflooding starts to decrease. This decrease is attributed to the increase in IFT (i.e., decrease in capillary number) in the second range, and increase in IFT and also pore plugging in the fourth range. Notwithstanding the decrease in capillary number for the surfactant waterflooding in the third range, increase in the oil recovery in this range (relative to the second range) is solely because of the pore blockage phenomenon.

Effect of monovalent ions (Na^+)

Fig. 10 shows the experimental ultimate oil recoveries for the waterflooding and consequent viscous-modified surfactant waterflooding versus NaCl concentration (at constant $MgCl_2$ and $CaCl_2$ concentrations of 0.5 wt.%). To confirm the trends, some of the experiments were repeated: the repeatability was acceptable (relative error in the range of 1.5–2.5%). As it is shown in Fig. 10, ultimate oil recovery for the waterflooding does not change noticeably by increasing NaCl concentration. In all these experiments

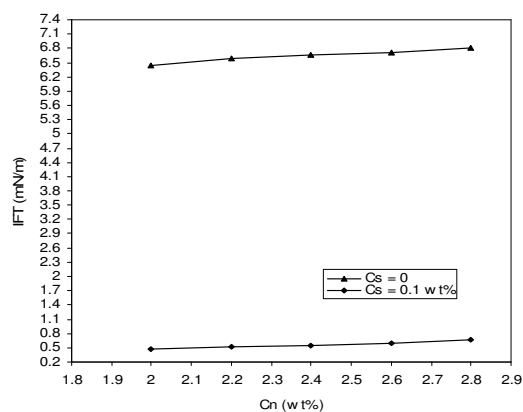


Fig. 11: Measured brine-oil and surfactant solution-oil IFT versus NaCl concentration ($MgCl_2$: 0.5 wt.%, $CaCl_2$: 0.5 wt.%). Concentrations of chemicals in polymer-surfactant solution in surfactant waterfloods are: surfactant = 0.10 wt.%, xanthan = 125 ppm, and ethanol = 0.75 wt.%.

no precipitation occurred as brine containing different NaCl concentrations were injected into the micromodel. Brine-crude oil IFT increases gradually by the increase in NaCl concentration (Fig. 11). Notwithstanding this gradual increase in brine-oil IFT, waterflooding recovery does not change noticeably. A gradual increase in brine-oil IFT and an increase in brine viscosity (Fig. 12) by increase in NaCl concentration canceled each other out. Thus, no remarkable change in the waterflooding recovery is seen by increasing NaCl concentration.

Fig. 10 also shows that the ultimate oil recovery for viscous-modified surfactant waterflooding decreases as NaCl concentration increases. Furthermore, Fig. 11 demonstrates that surfactant solution-oil IFT increases gradually by increasing NaCl concentration at a given concentration of $CaCl_2$ and $MgCl_2$ (0.5 wt.%). The decrease in ultimate oil recovery for surfactant waterflooding in Fig. 10 can be explained by the corresponding decrease in the capillary number (Fig. 13). No signs of precipitation and pore plugging in the micromodel were observed during the surfactant waterflooding by increasing NaCl concentration.

Wettability alteration in viscous-modified surfactant waterflooding

It is worth noting that wettability gradually changed when polymer-contained surfactant solution contacted the surface of the micromodel. Fig. 14a shows the initially

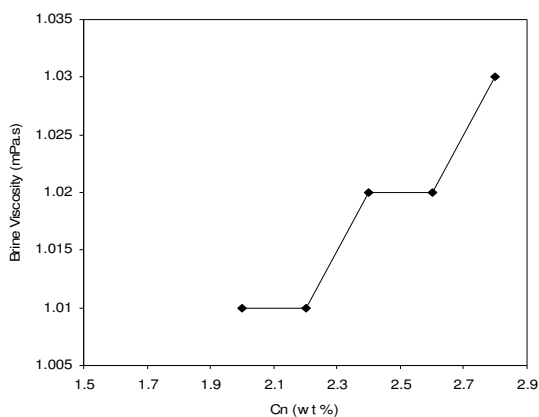


Fig. 12: Measured brine viscosity versus NaCl concentration ($MgCl_2$: 0.5 wt.%, $CaCl_2$: 0.5 wt.%).

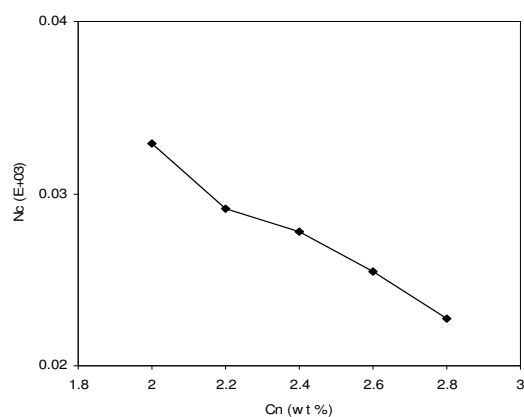


Fig. 13: Capillary number in viscous-modified surfactant waterflooding versus NaCl concentration ($MgCl_2$: 0.5 wt.%, $CaCl_2$: 0.5 wt.%). Concentrations of chemicals in polymer-surfactant solution in surfactant waterfloods are: surfactant = 0.10 wt.%, Xanthan = 125 ppm, and ethanol = 0.75 wt.%.

water-wet micromodel and the fluids (oil, connate water, and brine) distribution during one of the waterfloods conducted in this study. Fig. 14b shows the same portion of the micromodel and the distribution of fluids (oil, connate water, brine, and polymer-contained surfactant solution) during one of the viscous-modified surfactant waterfloods conducted in this study. Figs. 14a and 14b have been captured at the same spot in the micromodel. This enable us to compare the distribution of fluids during the waterflood and surfactant waterflood conducted in this study. A comparison between the distribution of fluids in pores and necks in Figs. 14a and 14b

clearly indicates that the wettability gradually shifted to an intermediate state (i.e., a less water-wet state) in Fig. 14b from an initially preferential water-wet state in Fig. 14a. Fig. 14a and 14b have been selected [among many captured images in this study] to show the typical distributions of the fluids during the waterfloods and surfactant waterfloods conducted in this study. The partial wettability change is an inalienable part of any surfactant-based displacement process. This phenomenon accompanies other working mechanisms such as IFT change, and surfactant portioning into the oleic phase (A comprehensive investigation of the mechanisms for the heavy oil recovery by surfactant-based chemical flooding has been conducted elsewhere [4–10]). Hence, based on the previous analysis, visual observation, and the microscopic inspection of the flow in the micromodel before, during, and after the surfactant waterfloods in this study, it is inferred that wettability shift has a minor effect on the heavy oil recovery trends in this study as compared to the effect of pore blockage.

Phenomenon of pore blockage during the viscous-modified surfactant waterflooding

It was mentioned that the pore blockage occurs in the third and fourth ranges of $CaCl_2$ concentration during the viscous-modified surfactant waterflooding (see Section of "Effect of divalent ions"). The pore blockage significantly influenced the ultimate oil recovery trends in the third and fourth ranges during the surfactant waterflooding. This phenomenon was captured by the digital camera during the surfactant waterflooding (see Fig. 15). Fig. 15 shows the blockage of some pore bodies in the middle of the captured image during the viscous-modified surfactant waterflooding in the third and fourth ranges of $CaCl_2$ concentration. Several instances of this kind of precipitation and pore blockage were observed in the third and fourth ranges of $CaCl_2$ concentration during the viscous-modified surfactant waterflooding. Fig. 15 has been selected [among many captured images in this study] to show the typical phenomenon of pore blockage during the surfactant waterfloods conducted in this study.

CONCLUSIONS

1. At low, intermediate, and high concentrations of Mg^{2+} , four different ranges for the effect of Ca^{2+} concentration exist for the viscous-modified surfactant waterflooding.

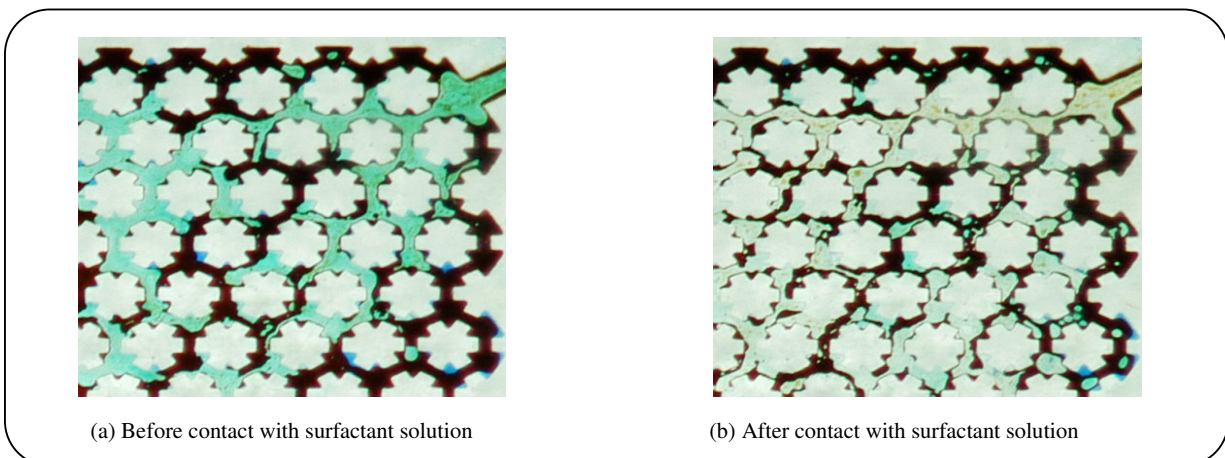


Fig. 14: Illustration of shift in wettability for micromodel (brown: oil, blue: connate water, green: waterflooding residue (brine), light grey: polymer-contained surfactant solution remained in the micromodel in the final state, white: grains). Concentrations of chemicals in polymer-surfactant solution in surfactant waterfloods are: surfactant = 0.10 wt.%, xanthan = 125 ppm, and ethanol = 0.75 wt.%.

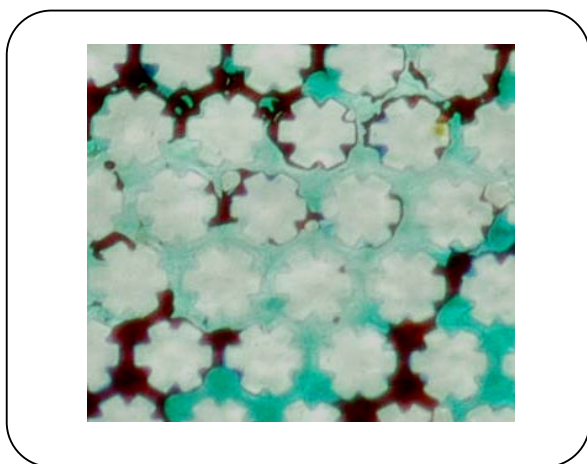


Figure 15. Illustration of the blockage of the some pore bodies in the middle of the captured image during the viscous-modified surfactant waterflooding in the third and fourth ranges of CaCl_2 concentration (brown: oil, blue: connate water, green: waterflooding residue (brine), light turquoise: sticky precipitate formed in the micromodel, white: grains). Concentrations of chemicals in polymer-surfactant solution in surfactant waterfloods are: surfactant = 0.10 wt.%, xanthan = 125 ppm, and ethanol = 0.75 wt.%.

2. In the first range of CaCl_2 concentration, surfactant performance is not adversely affected by the presence of CaCl_2 and the ultimate oil recovery does not change (tolerance range).

3. In the second range of CaCl_2 concentration,

ultimate oil recovery of viscous-modified surfactant waterflooding decreases due to the increase in IFT and decrease in capillary number.

4. Although third range of CaCl_2 concentration results in an increase of IFT, oil recovery increases (but never reaches the recovery in the first range) due to the effect of pore blockage phenomenon. In addition, under the experimental conditions in this study, the effect of wettability alteration on the trend of heavy oil recovery during the viscous-modified surfactant waterflooding is relatively minor as compared to the effect of pore blockage.

5. In the fourth range of CaCl_2 concentration, precipitation increases in such a way that more pore (even some pores with intermediate permeability) are plugged and thus, ultimate oil recovery decreases as CaCl_2 concentration increases.

6. The ultimate oil recovery decreases as the concentration of NaCl increases in the polymer-contained surfactant solution. The reason is an increase in surfactant solution-oil IFT and a decrease in capillary number because of the increase in NaCl concentration.

Acknowledgements

The first author is grateful to the Petroleum Research Center at the Petroleum University of Technology, Tehran, for providing the laboratory set-up and equipments, and the Research and Development Directorate of the National Iranian Oil Company for the financial support during conducting this research.

A major part of this paper is from the original Petroleum Society manuscript No. 2008-085 submitted for the 59th Annual Technical Meeting, Calgary, AB, 17-19 June 2008 and included on the Conference CD Proceedings. This material, as published by the Petroleum Society, is being used with permission from the Petroleum Society and the authors agree that copyright remains with the Petroleum Society for the material used in this article.

Nomenclature

C_c	Calcium chloride concentration
C_m	Magnesium chloride concentration
C_n	Sodium chloride concentration
P	Injection pressure, psi
S_{oi}	Initial oil saturation
T	Time, min
T	Temperature, °C
IFT	Interfacial tension, N.m ⁻¹
N_c	Capillary number

Received : Jane 23, 2009 ; Accepted : Apr. 25, 2010

REFERENCES

- [1] Yadali Jamaloei B., Insight Into the Chemistry of Surfactant-Based Enhanced Oil Recovery Processes. *Recent Patents Chem. Eng.*, **2**(1), p. 1 (2009).
- [2] Yadali Jamaloei, B., "Experimental Study of Surfactant/Water/Polymer Flooding Using One-Quarter Five-Spot Glass Micromodels", M.Sc. thesis. Petroleum University of Technology, Tehran, Iran (2007).
- [3] Yadali Jamaloei B., Kharrat R., Torabi F., Analysis and Correlations of Viscous Fingering in Low-Tension Polymer Flooding in Heavy Oil Reservoirs, *Energy & Fuels*, **24**(12), p. 6384 (2010).
- [4] Yadali Jamaloei B., Kharrat R., Fundamental Study of Pore Morphology Effect in Low Tension Polymer Flooding or Polymer-Assisted Dilute Surfactant Flooding, *Transp. Porous Media.*, **76**, p. 199 (2009).
- [5] Yadali Jamaloei B., Kharrat R., Analysis of Microscopic Displacement Mechanisms of Dilute Surfactant Flooding in Oil-Wet and Water-Wet Porous Media, *Transp. Porous Media*, **81**(1), p. 1 (2010).
- [6] Yadali Jamaloei B., Kharrat R., Analysis of Pore-Level Phenomena of Dilute Surfactant Flooding in the Presence and Absence of Connate Water Saturation, *J. Porous Media*, **13**(8), p. 671 (2010).
- [7] Yadali Jamaloei B., Kharrat R., The Influence of Pore Geometry on Flow Instability and Microscale Displacement Mechanisms of Dilute Surfactant Flooding in Mixed-Wet Porous Media, *J. Porous Media*, **14**(2), p. 91 (2011)
- [8] Yadali Jamaloei B., Ahmadloo F., Kharrat R., The Effect of Pore Throat Size and Injection Flowrate on the Determination and Sensitivity of Different Capillary Number Values at High-Capillary-Number Flow in Porous Media, *Fluid Dyn. Res.*, **42**(5), 055505 (2010).
- [9] Yadali Jamaloei B., Asghari K., Kharrat R., Ahmadloo F., Pore-Scale Two-Phase Filtration in Imbibition Process Through Porous Media at High- and Low-Interfacial Tension Flow Conditions, *J. Petrol. Sci. Eng.*, **72**(3-4), p. 251 (2010).
- [10] Yadali Jamaloei B., Kharrat R., Asghari K., Pore-Scale Events in Drainage Process Through Porous Media Under High- and Low-Interfacial Tension Flow Conditions, *J. Petrol. Sci. Eng.*, **75**(1-2), p. 223 (2010).
- [11] Yadali Jamaloei B., Kharrat R., Ahmadloo F., Selection of Proper Criteria in Flow Behavior Characterization of Low Tension Polymer Flooding in Heavy Oil Reservoirs, SPE Kuwait International Petroleum Conference and Exhibition, Kuwait City, Kuwait (2009).
- [12] Bansal V.K., Shah D.O., The Effect of Divalent Cations (Ca²⁺ and Mg²⁺) on the Optimal Salinity and Salt Tolerance of Petroleum Sulfonate and Ethoxylated Sulfonate Mixtures in Relation to Improved Oil Recovery, *J. Am. Oil Chem. Soc.*, **55**(3), p. 367 (1978).
- [13] Bansal V.K., Shah D.O., The Effect of Addition of Ethoxylated Sulfonate on Salt Tolerance, Optimal Salinity, and Impedence Characteristics of Petroleum Sulfonate Solutions, *J. Colloid Interface Sci.*, **65**(3), p. 451 (1978).
- [14] Glover C.J., Puerto M.C., Maerker J.M., Sandvik E.L., Surfactant Phase Behavior and Retention in Porous media, *Soc. Petrol. Eng. J.*, **19**(3), p. 183 (1979).
- [15] Gupta S.P., Trushenski S.P., Micellar Flooding-Compositional Effects on Oil Displacement, *Soc. Petrol. Eng. J.*, **19**(2), p. 116 (1979).
- [16] Hirasaki G.J., Application of the Theory of Multicomponent, Multiphase Displacement to Three-Component, Two-Phase Surfactant Flooding. *Soc. Petrol. Eng. J.*, **21**(2), p. 191 (1981).

- [17] Celik M.S., Manev E.D., Somasundaran P., Sulfonate Precipitation-Redissolution-Reprecipitation in Inorganic Electrolytes. In: Interfacial Phenomena in Enhanced Oil Recovery, *AIChE Symposium*, **212**(78), p. 86 (1982).
- [18] Hirasaki G.J., Lawson J.B., An Electrostatic Approach to the Association of Sodium and Calcium with Surfactant Micelles, *Soc. Petrol. Eng. Reservoir Eng.*, **1**(2), p. 119 (1986).
- [19] Nelson R.C., The Salinity Requirement Diagram—a Useful Tool in Chemical Flooding Research and Development, *Soc. Petrol. Eng. J.*, **22**(2), p. 259 (1982).
- [20] Kumar A., Neale G.H., Hornof V., Effects of Connate Water Composition on Interfacial Tension Behavior of Surfactant Solutions, *J. Can. Petrol. Tech.*, **23**(1), p. 37 (1984).
- [21] Kumar A., Neale G., Hornof V., Effects of Connate Water Ionic Composition on Coalescence of Oil Droplets in Surfactant Solutions, *J. Colloid Interface Sci.*, **104**(1), p. 130 (1985).
- [22] Maerker J.M., Gale W.W., Surfactant Flood Process Design for Loudon, *Soc. Petrol. Eng. Reservoir Eng.*, **7**(1), p. 36 (1992).
- [23] Novosad J., Surfactant Retention in Berea Sandstone—Effects of Phase Behavior and Temperature, *Soc. Petrol. Eng. J.*, **22**(6), p. 962 (1982).
- [24] Krumrine P.H., Falcone Jr., J.S., Campbell T.C., Surfactant Flooding 1: the Effect of Alkaline Additives on IFT, Surfactant Adsorption, and Recovery Efficiency, *Soc. Petrol. Eng. J.*, **22**(4), p. 503 (1982).
- [25] Dullien F.A.L., "Porous Media: Fluid Transport and Porous Structure", Academic Press, San Diego, CA (1992).
- [26] Zhong L., Mayer A., Glass R.J., Visualization of Surfactant-Enhanced Non-Aqueous Phase Liquid Mobilization and Solubilization in a Two Dimensional Micromodel, *Water Resour. Res.*, **37**(3), p. 523 (2001).
- [27] Morrow N.R., The Effects of Surface Roughness on Contact Angle with Special Reference to Petroleum Recovery., *J. Can. Petrol. Tech.*, **14**(4), p. 42 (1975).
- [28] Anderson W.G., Wettability Literature Survey-Part 2: Wettability Measurement, *J. Petrol. Tech.*, **38**(11), p. 1246 (1986).
- [29] Chatzis I., Kuntamukkula M.S., Morrow N.R., Effect of Capillary Number on the Microstructure of Residual Oil in Strongly Water-Wet Sandstones, *Soc. Petrol. Eng. Reservoir Eng.*, **3**(3), p. 902 (1988).
- [30] Friedmann F., Surfactant and Polymer Losses During Flow Through Porous Media, *Soc. Petrol. Eng. Reservoir Eng.*, **1**(3), p. 261 (1986).
- [31] Thibodeau L., Neale G.H., Effects of Connate Water on Chemical Flooding Processes in Porous Media, *J. Petrol. Sci. Eng.*, **19**(3-4), p. 159 (1998).
- [32] Emami Meybodi H., Kharrat R., Ghazanfari M.H., Effect of Heterogeneity of Layered Reservoirs on Polymer Flooding: an Experimental Approach Using Five-spot Glass Micromodel, EUROPEC/EAGE Conference and Exhibition, Rome, Italy (2008).